

Evidence for a mild steepening and Bottom-heavy IMF in Massive Galaxies from Sodium and Titanium-Oxide Indicators

C. Spiniello¹, S. C. Trager¹, L. V. E. Koopmans¹, Y. P. Chen¹

ABSTRACT

We measure equivalent widths (EW) – focussing on two unique features (NaI and TiO2) of low-mass stars ($\lesssim 0.3M_{\odot}$) – for luminous red galaxy spectra from the Sloan Digital Sky Survey (SDSS) and X-Shooter Lens Survey (XLENS) in order to study the low-mass end of the initial mass function (IMF). We compare these EWs to those derived from simple stellar population models computed with different IMFs, ages, $[\alpha/\text{Fe}]$, and elemental abundances. We find that models are able to simultaneously reproduce the observed NaD $\lambda 5895$ and Na I $\lambda 8190$ features for lower-mass ($\sim \sigma_*$) early-type galaxies (ETGs) but deviate increasingly for more massive ETGs, due to strongly mismatching NaD EWs. The TiO2 $\lambda 6230$ and the Na I $\lambda 8190$ features together appear to be a powerful IMF diagnostic, with age and metallicity effects orthogonal to the effect of IMF. We find that both features correlate strongly with galaxy velocity dispersion. The XLENS ETG (SDSSJ0912+0029) and an SDSS ETG (SDSSJ0041-0914) appear to require both an extreme dwarf-rich IMF and a high sodium enhancement ($[\text{Na}/\text{Fe}] = +0.4$). In addition, lensing constraints on the total mass of the XLENS system within its Einstein radius limit a bottom-heavy IMF with a power-law slope to $x \leq 3.0$ at the 90% C.L. We conclude that NaI and TiO features, in comparison with state-of-the-art SSP models, suggest a mildly steepening IMF from Salpeter ($dn/dm \propto m^{-x}$ with $x = 2.35$) to $x \approx 3.0$ for ETGs in the range $\sigma = 200 - 335 \text{ km s}^{-1}$.

Subject headings: dark matter — galaxies: elliptical and lenticular, cD — gravitational lensing: strong — galaxies: kinematics and dynamics — galaxies: evolution — galaxies: structure

1. Introduction

When constraining the star formation, metallicity and gas/dust content of galaxies, the initial mass function (IMF) is often assumed to be universal and equal to that of the

¹Kapteyn Institute, University of Groningen, PO Box 800, 9700 AV Groningen, the Netherlands

solar neighborhood (Kroupa 2001; Chabrier 2003; Bastian, Covey & Meyer 2010). However, evidence has recently emerged that the IMF might evolve (Davé 2008; van Dokkum 2008) or depend on the stellar mass of the system (e.g. Worthey 1992; Trager et al. 2000b; Graves et al. 2009; Treu et al. 2010; Auger et al. 2010b; Napolitano 2010; van Dokkum & Conroy 2010). van Dokkum & Conroy (2010; hereafter vDC10) suggested that low-mass stars ($\leq 0.3 M_{\odot}$) could be more prevalent in massive early-type galaxies. The increase in the mass-to-light ratio (M/L) of galaxies with galaxy mass may thus be partly due to a changing IMF rather than an increasing dark matter fraction, consistent with previous suggestions (Treu et al. 2010, Auger et al. 2011, Barnabè et al. 2011, Dutton et al. 2012, Cappellari et al. 2012). vDC10 showed that some spectral features, such as the Na I $\lambda\lambda 8183, 8195$ doublet (called NaI0.82 by CvD12), depend strongly on surface gravity at fixed effective temperature, betraying the presence of faint M dwarfs in integrated light spectra. If correct, the low-mass end of the IMF can be inferred directly from red/near-IR spectra of old populations. Hence, the strength of the Na I doublet versus another sodium feature, such as the NaD doublet (called Na0.59 by CvD12), should provide a powerful means for separating the IMF from other effects. Specifically for the purpose of determining the low-mass IMF down to $\sim 0.1 M_{\odot}$ for metal-rich stellar populations with ages of 3–13.5 Gyr, Conroy & van Dokkum (2012; hereafter CvD12) presented new population synthesis models. The NaD feature responds more strongly to Na-enhancement than IMF in the CvD12 models, while the Na I doublet is strong in stars with mass $< 0.3 M_{\odot}$ and weak or absent in all other types of stars. Unfortunately, NaI0.82 is also sensitive to age and metallicity, and NaD is influenced by any interstellar medium. It is therefore necessary to test these models over a range of age and metallicity indicators, as well as against other lines caused by low-mass stars.

In this letter, we focus on the NaI feature as indicator of low-mass stars. We use NaD as indicator of a change in sodium abundance and $H\beta$ and $[\text{MgFe}]$ as indicators of age and metallicity, respectively. This allows us to assess model degeneracies and deficiencies. We propose the use of the TiO feature at $\lambda 6230$ as an indicator of the presence of low-mass stars. We find that both of these features (NaI and TiO) correlate with galaxy velocity dispersion, implying a steepening of the IMF slope in ETGs with $\sigma > \sigma_*$. We assume $H_0 = 70 \text{ km s}^{-1} \text{ Mpc}^{-1}$, $\Omega_m = 0.3$ and $\Omega_{\Lambda} = 0.7$ throughout this letter.

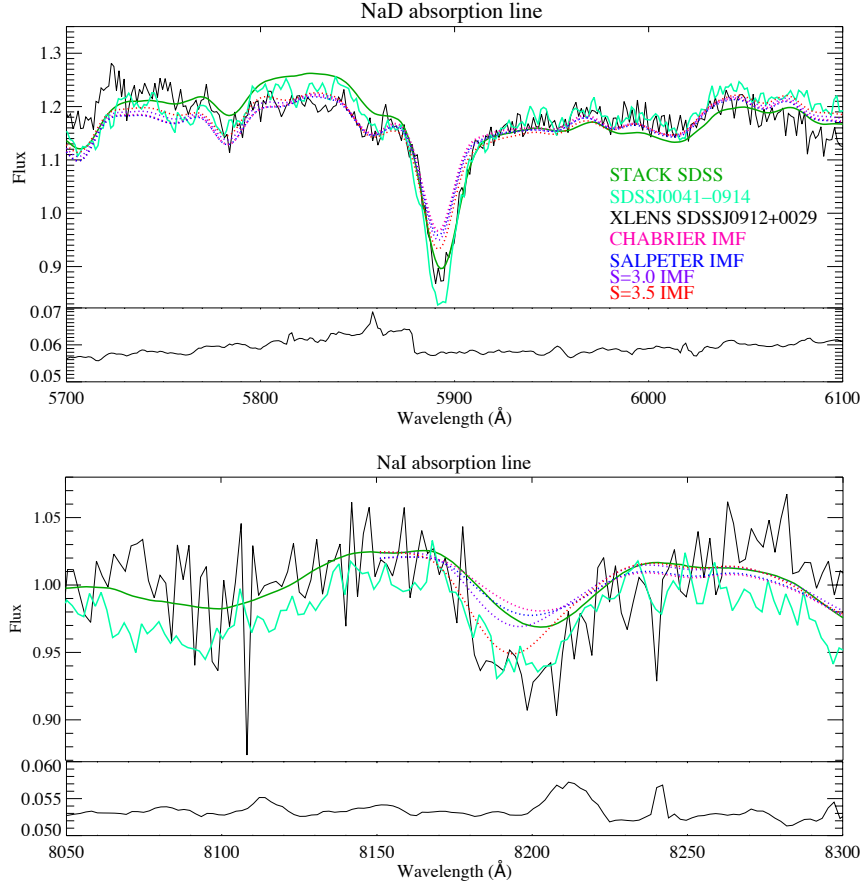


Fig. 1.— Galaxy (continuous lines) and model (dashed lines) spectra in the regions of the NaD (top) and NaI (bottom) features. The observed NaD EWs do not match the models for the most massive ETGs ($\geq 300 \text{ km s}^{-1}$). Na I absorption is stronger in the XLENS system and SDSSJ0041-0914 and appears in both cases to require an IMF steeper than Salpeter, while the stacked SDSS spectrum shows a weaker Na I feature that matches a model with a Salpeter IMF. The bottom panels show the noise spectrum of the XLENS system.

2. The data

As part of the XLENS¹ project, we obtained a UVB-VIS X-shooter spectrum of the massive and luminous early-type SLACS (Sloan Lens ACS Survey, Bolton et al. 2006) lens galaxy SDSS J0912+0029 at $z = 0.1642$, with high enough signal-to-noise to perform stellar population analyses. The lens galaxy shows a surprisingly deep NaI0.82 feature (Fig.1), making it an extremely interesting target for studying the low-mass end of the IMF in ETGs. We measure the luminosity-weighted velocity dispersion of the lens galaxy from the reduced flux-calibrated 1D UVB–VIS spectrum using the Penalized Pixel Fitting (pPXF) code of Cappellari & Emsellem (2004). We obtain $\langle\sigma_*\rangle(\lesssim R_{\text{eff}}) = 325 \pm 10 \pm 12 \text{ km s}^{-1}$, in agreement with the previously published value ($\sigma \simeq 313 \pm 12 \text{ km s}^{-1}$; Bolton et al. 2006). We also used the spectra of ~ 250 galaxies with similar morphology and colors (all LRGs) from the Sloan Digital Sky Survey DR8 (SDSS; Aihara et al. 2011), in five velocity-dispersion bins spread over $200\text{--}335 \text{ km s}^{-1}$ (~ 50 galaxies per bin). We examine one system, SDSSJ0041-0914, separately because it has a NaI0.82 feature comparably deep to the XLENS system.

3. Stellar Population Synthesis Modeling

We use the synthetic spectra of CvD12 to analyze the stellar populations of these galaxies. The models make use of two separate empirical libraries, the MILES library covering $3500\text{--}7400 \text{ \AA}$ (Sánchez-Blázquez et al. 2006) and the IRTF library of cool stars covering $8100\text{--}24000 \text{ \AA}$ (Cushing et al. 2005; Rayner et al. 2009). They also incorporate synthetic spectra with the purpose of investigating changes in the overall metallicity or changes in the abundances of individual elements and to cover the gap in wavelength between the two empirical libraries. We refer to CvD12 for details. The abundance variations of single elements are implemented at fixed $[\text{Fe}/\text{H}]$, which implies that the total metallicity Z varies from model to model. We measure line-strength indices in the range $4000\text{--}8400 \text{ \AA}$, including the standard Lick indices $H\beta$, Mgb , $\text{Fe}5270$, $\text{Fe}5335$, NaD and a TiO index ($\text{TiO}2$) using the definitions of Trager et al. (1998), and the commonly-used $[\text{MgFe}]$ combination².

We define a modified index around the Na I doublet $8183, 8195 \text{ \AA}$, which seems to be strongly dependent on the low-mass end of the IMF (Table 1). This index is slightly different from that used by vDC10 and CvD12, having a wider central index bandpass and slightly wider pseudo-continua. Our definition is more stable against velocity dispersion variations

¹The X-Shooter Lens Survey, Spiniello et al. (2011)

² $[\text{MgFe}] = \sqrt{(\text{Fe}5270 + \text{Fe}5335)/2} \times \text{Mgb}$, González (1993)

and more suitable for massive ETGs. We convolve all the galaxy and model spectra to an effective velocity dispersion of $\sigma = 335 \text{ km s}^{-1}$ (the upper limit in our sample), to correct for kinematic broadening, before measuring indices. Indices in both the observed and synthetic spectra are measured with the same definitions and method (SPINDEX2; Trager et al. 2008). We do not place our indices on the zero-point system of the Lick indices and quote them as equivalent widths (EWs) in units of \AA , except for TiO2, which is given in magnitudes.

4. Results and discussion

$H\beta$ is primarily an age indicator, while a combination of Mgb , $Fe5270$, and $Fe5335$ yields information on the mean metallicity $[Z/H]$ of the population (Worthey 1994) while minimizing the effects of abundance ratio variations (e.g., González 1993; Trager et al. 2000a). These indices (Panel (a), Fig. 2) show a good agreement between the models and the galaxies EWs for old stellar populations, with an age of $13.5 \pm 3 \text{ Gyr}$ for $\sigma \geq 300 \text{ km s}^{-1}$ (black points) and younger ages for lower mass ETGs. The statistical error is deduced directly from variations in $H\beta$ ³. The most massive ETGs have values of $[\alpha/Fe]$ between solar and super-solar (~ 0.2), in good agreement with the prediction that massive galaxies have significantly super-solar abundance ratios because of rapid, high-efficiency star formation (Trager et al. 2000b; Thomas et al. 2005, Spolaor et al. 2009, 2010). Given the uncertainties in the line-strengths of the two individual galaxies (SDSSJ0912+0029 and SDSSJ0041-0914), we are unable to determine their ages and metallicities precisely, but their line strengths are similar to the mean of the highest-mass SDSS sample, with a deviation from the average EW smaller than 1σ in both age and metallicity. The NaI and NaD indices can in principle be used to

³For stellar populations with ages $> 10 \text{ Gyr}$, an uncertainty of 0.1 \AA in $H\beta$ corresponds to 1 Gyr uncertainty in the age (cf. Worthey 1994).

Table 1. Definition of the index around the Na I doublet 8183, 8195 \AA

Index	Central band (\AA)	Pseudocontinua (\AA)
NaI	8168.500 – 8234.125	8150.000 – 8168.400 8235.250 – 8250.000

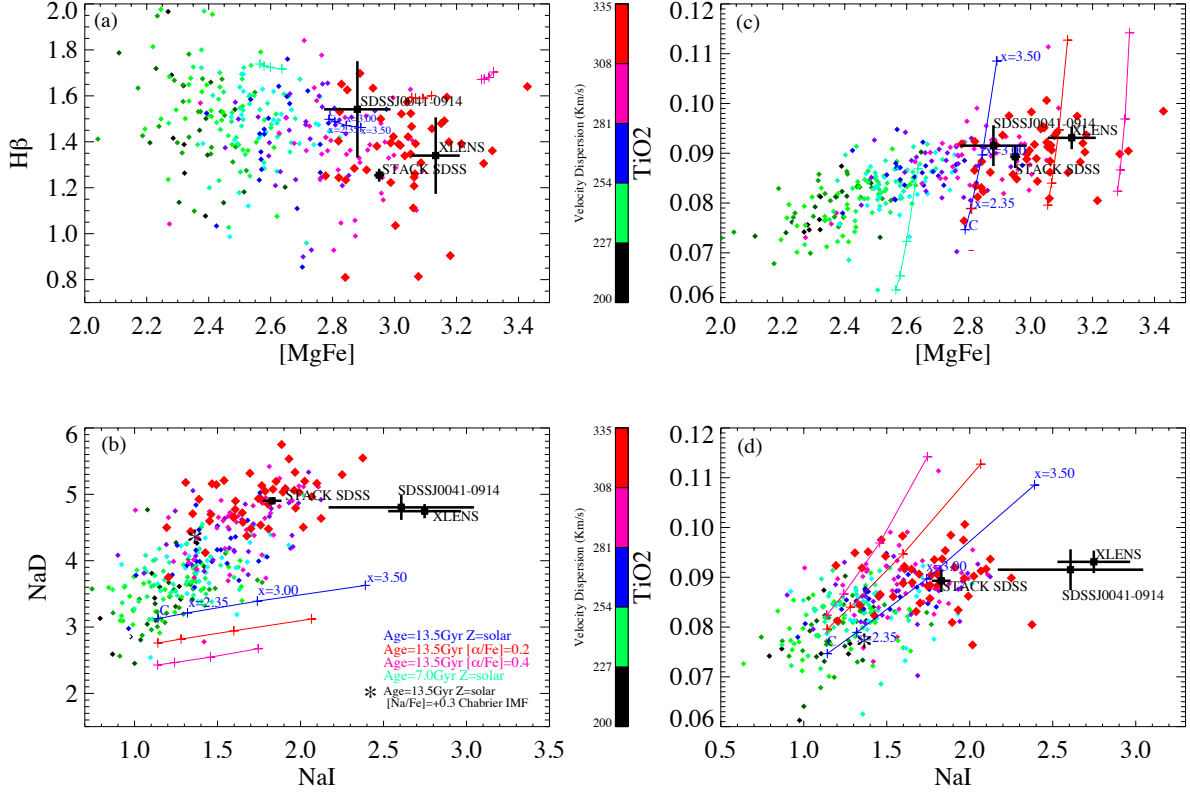


Fig. 2.— Index-index plots of the main absorption features. Lines and crosses are different SSP models from CvD12 with increasing IMF (Chabrier, Salpeter with a slope of $x = 2.35$, a bottom-heavy IMF with slope of $x = 3.0$ and an extremely dwarf-rich IMF with a slope of $x = 3.5$). Points colored according to their velocity dispersions are individual SDSS galaxies, with index errors similar to SDSS J0041-0914. In the plots showing sodium, the XLENSS system SDSSJ0912+0029 requires a very steep IMF, violating lensing constraints on its total mass (see the text for further details). *Panel (a)*: $H\beta$ as a function of $[MgFe]$. The most massive ETGs ($> 300 \text{ km s}^{-1}$) best match an old stellar population (13.5 Gyr) with super-solar total metallicity. Lower-mass systems are younger. *Panel (b)*: NaD as a function of NaI . Only low-mass ($< 250 \text{ km s}^{-1}$) systems match the models. More massive ETGs require a higher $[Na/Fe]$ and the XLENSS system and SDSSJ0041-0914 also require a very steep IMF slope. *Panel (c)*: $TiO2$ as a function of $[MgFe]$. The most massive ETGs require an IMF slope slightly steeper than Salpeter. A Chabrier-type IMF systematically underestimates the SDSS $TiO2$ EWs. *Panel (d)*: $TiO2$ as a function of NaI . The ETGs match with the models using a Salpeter or slightly steeper IMF, but the XLENSS system and SDSSJ0041-0914 still do not match the SSP models well.

constrain the IMF slope (CvD12), and this relation is shown in Figure 2b. Although the data match the models for low-dispersion systems ($\lesssim 250 \text{ km s}^{-1}$), the models with solar $[\text{Na}/\text{Fe}]$ abundance do not match the NaD strengths and only models with $[\text{Na}/\text{Fe}] = +0.3 - +0.4$ dex match the NaD indices for higher-mass ETGs. We suggest two possible explanations for this behavior:

(i) NaD is highly contaminated by the interstellar medium (ISM) for higher mass ETGs; for example, dust lanes provide additional absorption in this resonance line (Sparks et al. 1997). Interstellar absorption within a galaxy may alter the stellar absorption profile and therefore the calculated EW, leading to an incorrect inference of the underlying stellar population.

(ii) Very massive ETGs have higher $[\text{Na}/\text{Fe}]$ abundances (> 0.3 dex) *and* slightly bottom-heavy IMFs which correlate with their stellar velocity dispersions. Therefore, if we explain the strengths of these features in giant ETGs using abundance ratios, we require an average iron abundance in excess of solar ($[\text{Fe}/\text{H}] \sim 0.2$), a IMF with $x = 3.0$ and a high sodium abundance ($[\text{Na}/\text{H}] > 0.3$). In the α -enhanced bulge of the Galaxy, Fulbright et al. (2006) find an averaged $[\text{Na}/\text{Fe}] = 0.2$ dex, and that $[\text{Na}/\text{Fe}] \leq 0.3$ dex in all stars. However, Lecureur et al. (2007) find that $[\text{Na}/\text{Fe}]$ ratios increase sharply with metallicity. They obtain values of $[\text{Na}/\text{Fe}] \sim 0.5$ for $[\text{Fe}/\text{H}] = 0$ and even higher for $[\text{Fe}/\text{H}] > 0$, but with a scatter of 0.29 dex resulting in a range of $[\text{Na}/\text{Fe}]$ from -0.1 to almost 1.0. It is therefore possible for massive ellipticals to have high $[\text{Na}/\text{Fe}]$. In both cases, the models seem consistent with a Salpeter IMF at the low-dispersion end and a slightly bottom-heavy IMF for the high-dispersion end, if these effects are accounted for, but the models predict a steeper IMF slope of $x \sim 3.0 - 3.5$ for both the XLENs galaxy SDSSJ0912+0029 and SDSSJ0041-0914.

We note that a TiO feature at 8199 \AA could partly contaminate NaI, although this feature should not vary strongly (CvD12). To test possible contamination, we use a model with $[\text{Ti}/\text{Fe}] = \pm 0.3$ and calculate the NaI EW for a Chabrier IMF. We find that Ti enhancement only affect the NaI index by 1%.

Overall we conclude that the NaD EWs and its trend with stellar mass remain unexplained for systems with $\sigma \gtrsim 250 \text{ km s}^{-1}$. We find that SSP models predict that TiO features also depend strongly on the slope of the low-mass end of the IMF, such as TiO2, shown in Figures 2c and 2d. This indicator gives more support to the conclusion that the sodium strengths of the XLENs ETG, SDSSJ0912+0029, still remain somewhat difficult to explain by current stellar population models, although most SDSS systems can be matched in NaI for most ETGs (if not in NaD). Together the TiO2 and NaI indices both imply a bottom-heavy IMF, steepening from Salpeter to possibly $x \approx 3$ for the most massive SDSS ETGs.

As in Treu et al. (2010), a bottom-light IMF such as Chabrier IMF is inappropriate for the most massive ETGs.

4.1. Limits on the IMF from Strong Lensing

A strong case against an extreme bottom-heavy IMF can be made using the system with the strongest NaI EW (Fig. 2), the XLENS galaxy SDSSJ0912+0029. This system provides a hard upper limit on the stellar mass inside its Einstein radius, no matter the IMF model. If we assume that the SSP models are correct and that this galaxy has a high [Na/Fe] abundance, we infer an IMF with a power-law slope $x = 3\text{--}3.5$ (where the IMF follows $dn/dm = m^{-x}$, and the Salpeter slope is $x = 2.35$). To assess whether these steep IMF slopes are consistent with the upper limit on the total mass, we calculate the total luminosity and the SSP stellar M/L ratio in stars for each assumed IMF to infer the stellar mass fraction inside the Einstein radius ($R_{\text{Ein}} = 4.55 \pm 0.23 \text{ kpc}$; Koopmans et al. 2006). Changes in the IMF of stars with $M \leq 0.3 M_{\odot}$ changes the total luminosity of the lens galaxy by at most $\sim 10\%$. Conversely, stars with masses of $0.1\text{--}0.3 M_{\odot}$ contribute $\gtrsim 60\%$ of the stellar mass for bottom-heavy IMFs with slopes steeper than Salpeter (see, e.g., Fig. 2 of CvD12). To determine the stellar M/L ratio, we use the isochrones at solar [Fe/H] and $[\alpha/\text{H}]$ for a 13.5 Gyr population from the Dartmouth Stellar Evolution Program (DSEP), a state-of-the-art stellar evolution code (Chaboyer, Green, & Liebert 1999; Chaboyer et al. 2001). We compare three different IMFs: Salpeter ($x = 2.35$), a bottom-heavy IMF ($x = 3.0$) and a very bottom-heavy IMF ($x = 3.5$). CvD12 use the same isochrones in their SSP for the bulk of the main sequence and red giant branch, except at $M < 0.2 M_{\odot}$, where they use the Baraffe et al. (1998) isochrones. For each IMF we compute the quantity

$$f_{\text{Ein}}^* = M^*/M_{\text{Ein}} = (L_{\text{Ein}}/M_{\text{Ein}}) \times (M_*/L)_{\text{DSEP}},$$

where M_{Ein} is a robust measurement of the total mass enclosed within the physical Einstein radius [$M_{\text{Ein}} = (39.6 \pm 0.8) \times 10^{10} M_{\odot}$], L_{Ein} is the luminosity enclosed within the Einstein radius, evaluated using B-spline luminosity models, as a fraction of de Vaucouleurs total model luminosity [$L_{\text{Ein}} = (4.49 \pm 0.2) \times 10^{10} L_{\odot}$, from Bolton et al. 2008], and $(M_*/L)_{\text{DSEP}}$ is the mass-to-light ratio from the DSEP isochrone using the appropriate IMF. The stellar M/L ratio includes the contribution from stellar remnants and gas ejected from stars at the end of their life-cycles. We list the results of this calculation in Table 2. For a Salpeter IMF, the stellar mass fraction of SDSSJ0912+0029 in the restframe V -band is $f_{\text{Ein,Salp}}^* = 0.59 \pm 0.15$, in agreement with previous results (0.60 ± 0.09 , Auger et al. 2009). The mass-to-light ratio calculated from the DSEP isochrone for a Salpeter IMF is $M/L_V = 7.2 \pm 2 (M/L)_{\odot}$ in the V band and $M/L_B = 10.2 \pm 3 (M/L)_{\odot}$ in the B band. The latter value is consistent with

Table 2. Variation with IMF of M/L and stellar mass fraction within the Einstein radius

IMF slope ($dN/dm = M^\gamma$)	$(M/L)_{DSEP,B}^*$ ($[\alpha/Fe] = 0.0$)	$(M/L)_{DSEP,V}^*$ ($[\alpha/Fe] = 0.0$)	f_B^* ($L_{\text{Ein}}/M_{\text{Ein}}\text{)} \times (M/L)_B^*$	f_V^* ($L_{\text{Ein}}/M_{\text{Ein}}\text{)} \times (M/L)_V^*$
2.35	10.2 ± 3	7.2 ± 2	0.75 ± 0.2	0.59 ± 0.18
3.00	22 ± 6	16 ± 5	1.6 ± 0.5	1.4 ± 0.4
3.50	43 ± 13	29 ± 9	2.4 ± 0.8	2.4 ± 0.7

Note. — The constraints on the mass and luminosity within the Einstein radius are taken from Auger et al. (2009) and Barnabè et al. (2009). All quantities are calculated in the rest-frame V- and B-band.

the upper limit of $M/L_B \leq 9.08 (M/L)_\odot$ derived from dynamical models of Barnabè et al. (2009) under the maximum bulge hypothesis. An IMF slope of $x = 3.5$ yields $M/L_V = 29 \pm 9 (M/L)_\odot$, and $M/L_B = 43 \pm 13 (M/L)_\odot$ corresponding to $f_{\text{Ein},3.5}^* = 2.4 \pm 0.8$, inconsistent with the total lensing mass within the Einstein radius at the $> 95\%$ confidence level. An IMF of $x = 3.0$ in B -band is also excluded at the $> 90\%$ level, as this corresponds to a fraction $f_{\text{Ein},3.0,B}^* = 1.6 \pm 0.5$. For both of the bottom heavy IMFs in B -band and for the $x = 3.5$ IMF in V -band, we obtain a stellar mass fraction within the Einstein radius in excess of unity, thereby violating the lensing constraint on the total mass of the system at the $> 90\%$ CL. The $x = 3$ model is only marginally consistent in V -band, but $f_{\text{Ein},3.0,V}^* = 1.4 \pm 0.4$ implies that there is no dark matter within the Einstein radius.

4.2. Systematic uncertainties

The uncertainty on the value of f_{Ein}^* has a number of contributions. The uncertainties in the mass and luminosity determinations from lensing are much smaller than differences in the values of M/L arising from the use of different stellar population evolution models. The emerging picture is that, for a fixed IMF, it is difficult to constrain M/L estimates to much higher accuracy than 0.1 dex (Gallazzi et al. 2008; Marchesini et al. 2009; Longhetti & Saracco 2009, Conroy et al. 2009, 2010). We examine mass-to-light ratios predicted for different IMF from different stellar population models in the rest-frame V - and B -bands and compare predictions from Worthey (1994), Bruzual & Charlot (2003), Maraston (2005), and Vazdekis et al. (2010) for single stellar populations with ages 11.2–14.1 Gyr, solar ($Z = 0.02$) or super-solar metallicity ($Z = 0.05$). For each SSP and each IMF, we calculate an average value and a standard deviation that we associate with the inferred values of M/L . Changing the $[\text{Fe}/\text{H}]$ abundance from 0 to 0.22 yields a $\sim 9\%$ uncertainty on M/L , while changing the age of the stellar population changes M/L by $\sim 20\%$ at fixed IMF. The latter is the dominant contribution to the final uncertainties. We propagated these errors into the stellar mass fraction. The errors on the stellar mass fractions in Table 2 include both the random error contribution and the systematic uncertainties due to the use of different set of isochrones, bands, and stellar population age and metallicity uncertainties.

5. Conclusions

In this letter we have studied the Na I $\lambda 8190$ and TiO $\lambda 6230$ features – both indicators of low-mass ($< 0.3 M_\odot$) stars in massive ETGs – as a function of each other, of age and metallicity indicators (Mgb, Fe, H β), of NaD, and of stellar velocity dispersion. We find the

following: (1) The observed NaI-NaD trend depends strongly on stellar velocity dispersion of ETGs and only match current state-of-the-art SSP models for ETGs with $\sigma \lesssim 250 \text{ km s}^{-1}$. The most extreme NaI index strength in our sample is found in a gravitational lens system, which should have an IMF slope $x \gtrsim 3$ based on the best current SSP models. The total enclosed mass of this system, however, excludes slopes steeper than $x = 3.0$ at the $> 90\%$ CL or slopes steeper than $x = 3.5$ at the $> 95\%$ CL. We conclude that the NaD feature is still affected by as-of-yet not understood processes in the more massive ETGs ($\sigma > 250 \text{ km s}^{-1}$). A full spectral comparison, in combination with lensing and dynamical constraints, is planned to further strengthen these results and assess whether NaI and NaD (in some instances) are contaminated. (2) We find that the TiO feature at $\lambda \sim 6230 \text{ \AA}$ (TiO2) is a particularly promising feature to decouple the IMF from age, metallicity, and abundance pattern of the stellar population, especially when combined with metallicity-dependent indices. We find that this feature correlates well with NaI, if the two most extreme cases as discussed in the text, are excluded. This correlation can be a crucial piece of evidence against interstellar contamination of the Na I $\lambda 8190$ sodium absorption lines, although this does not solve the problem of NaD absorption. If strong NaI features are indeed not due to ISM contamination, very massive ETGs have higher [Na/Fe] abundances (> 0.3 dex) *and* slightly bottom-heavy IMFs, correlated with their stellar velocity dispersions. We also find a clear trend of an increasing IMF slope between $\sigma = 200$ to 335 km s^{-1} from Salpeter ($x = 2.35$) to $x \approx 3.0$, in agreement with the XLENS system, which excludes steeper IMFs at the high-mass end.

Our results are the first SSP-based indications of a steepening of the low-mass end of the IMF with increasing galaxy mass *within* the class of LRG/ETGs. Our results (i) support a similar trend first found by Treu et al. (2010), (ii) extend the evidence based on SSP models that the IMF steepens from spiral to early-type galaxies (vDC10), (iii) suggest that NaI and NaD (in some instances) could be contaminated by interstellar absorption, and (iv) support a similar trend found by Cappellari et al. (2012) based on stellar kinematics. The upper limit of $x \lesssim 3$, based on one of the most massive ETGs in our sample, a gravitational lens, also supports our previous similar finding (Spiniello et al. 2011).

Acknowledgements

The authors thank the referee for providing constructive comments. Data were reduced using EsoRex and the XSH pipeline developed by the ESO Data Flow System Group. C.S. acknowledges support from an Ubbo Emmius Fellowship. L.V.E.K. is supported in part by an NWO-VIDI program subsidy (project number 639.042.505). The authors thank C. Conroy and P. van Dokkum for kindly providing their stellar population models before publication

and for providing very useful feedback on a draft manuscript that helped to improve it. The authors thank T. Treu and M. den Brok for useful comments on the manuscript.

REFERENCES

- Aihara, H., Allende Prieto, C., An, D., et al. 2011, *ApJS*, 193, 29
- Auger, M. W., Treu, T., Bolton, A. S., et al. 2009, *ApJ*, 705, 1099
- Auger, M. W., Treu, T., Gavazzi, R., et al. 2010, *ApJ*, 721, L163
- Auger, M. W., Treu, T., Bolton, A. S., et al. 2010, *ApJ*, 724, 511
- Baraffe, I., Chabrier, G., Allard, F., & Hauschildt, P. H. 1998, *A&A*, 337, 403
- Barnabè, M., Czoske, O., Koopmans, L. V. E., et al. 2009, *MNRAS*, 399, 21
- Barnabè, M., Czoske, O., Koopmans, L. V. E., Treu, T., & Bolton, A. S. 2011, *MNRAS*, 415, 2215
- Bastian, N., Covey, K. R., & Meyer, M. R. 2010, *ARA&A*, 48, 339
- Bolton, A. S., Burles, S., Koopmans, L. V. E., Treu, T., & Moustakas, L. A. 2006, *ApJ*, 638, 703
- Bolton, A. S., Burles, S., Koopmans, L. V. E., et al. 2008, *ApJ*, 682, 964
- Bruzual, G., & Charlot, S. 2003, *MNRAS*, 344, 1000
- Cappellari, M., & Emsellem, E. 2004, *PASP*, 116, 138
- Cappellari, M., McDermid, R. M., Alatalo, K., et al. 2012, arXiv:1202.3308
- Chaboyer, B., Green, E. M., & Liebert, J. 1999, *AJ*, 117, 1360
- Chaboyer, B., Fenton, W. H., Nelan, J. E., Patnaude, D. J., & Simon, F. E. 2001, *ApJ*, 562, 521
- Chabrier, G. 2003, *PASP*, 115, 763
- Conroy, C., Gunn, J. E., & White, M. 2009, *ApJ*, 699, 486
- Conroy, C., White, M., & Gunn, J. E. 2010, *ApJ*, 708, 58

- Conroy, C., & van Dokkum, P. 2012, *ApJ*, 747, 69
- Cushing, M. C., Rayner, J. T., & Vacca, W. D. 2005, *ApJ*, 623, 1115
- Davé, R. 2008, *MNRAS*, 385, 147
- Dutton, A. A., Mendel, J. T., & Simard, L. 2012, *MNRAS*, L412
- Fulbright, J. P., Rich, R. M., & McWilliam, A. 2006, *Chemical Abundances and Mixing in Stars in the Milky Way and its Satellites*, 93
- Gallazzi, A., Brinchmann, J., Charlot, S., & White, S. D. M. 2008, *MNRAS*, 383, 1439
- Graves, G. J., Faber, S. M., & Schiavon, R. P. 2009, *ApJ*, 698, 1590
- González, J. J. 1993, Ph.D. Thesis,
- Koopmans, L. V. E., Treu, T., Bolton, A. S., Burles, S., & Moustakas, L. A. 2006, *ApJ*, 649, 599
- Kroupa, P. 2001, *MNRAS*, 322, 231
- Lecureur, A., Hill, V., Zoccali, M., et al. 2007, *A&A*, 465, 799
- Longhetti, M., & Saracco, P. 2009, *MNRAS*, 394, 774
- Maraston, C. 2005, *MNRAS*, 362, 799
- Marchesini, D., van Dokkum, P. G., Förster Schreiber, N. M., et al. 2009, *ApJ*, 701, 1765
- Napolitano, N. R., Romanowsky, A. J., & Tortora, C. 2010, *MNRAS*, 405, 2351
- Rayner, J. T., Cushing, M. C., & Vacca, W. D. 2009, *ApJS*, 185, 289
- Sanchez-Blazquez, P., Peletier, R. F., Jimenez-Vicente, J., et al. 2007, *VizieR Online Data Catalog*, 837, 10703
- Sparks, W. B., Carollo, C. M., & Macchetto, F. 1997, *ApJ*, 486, 253
- Spiniello, C., Koopmans, L. V. E., Trager, S. C., Czoske, O., & Treu, T. 2011, *MNRAS*, 417, 3000
- Spolaor, M., Hau, G. K. T., Forbes, D. A., & Couch, W. J. 2010, *MNRAS*, 408, 254
- Spolaor, M., Proctor, R. N., Forbes, D. A., & Couch, W. J. 2009, *ApJ*, 691, L138

- Thomas, D., Maraston, C., Bender, R., & Mendes de Oliveira, C. 2005, *ApJ*, 621, 673
- Trager, S. C., Worthey, G., Faber, S. M., Burstein, D., & Gonzalez, J. J. 1998, *ApJS*, 116, 1
- Trager, S. C., Faber, S. M., Worthey, G., & González, J. J. 2000, *AJ*, 119, 1645
- Trager, S. C., Faber, S. M., Worthey, G., & González, J. J. 2000, *AJ*, 120, 165
- Trager, S. C., Faber, S. M., & Dressler, A. 2008, *MNRAS*, 386, 715
- Treu, T., Auger, M. W., Koopmans, L. V. E., et al. 2010, *ApJ*, 709, 1195
- van Dokkum, P. G. 2008, *ApJ*, 674, 29
- van Dokkum, P. G., & Conroy, C. 2010, *Nature*, 468, 940
- Vazdekis, A., Sánchez-Blázquez, P., Falcón-Barroso, J., et al. 2010, *MNRAS*, 404, 1639
- Worthey, G. 1992, *The Stellar Populations of Galaxies*, 149, 507
- Worthey, G. 1994, *ApJS*, 95, 107